Modeling of field emission from laser etched porous silicon

H. R. Dehghanpour *

Dept. of Physics, Tafresh University, Tafresh, Iran

** Corresponding author: hamid.r.dehghanpour@gmail.com*

Abstract

In many modern sciences, electron transfer is required, such as electron microscopes, microwaves, and screens. There have been numerous reports of the formation of microstructures on silicon surfaces using lasers in halogen-containing media and their optical, electrical and other physical properties. A silicon microstructured field emitter is modeled with Fowler-Nortium field diffusion theory, and the breakdown currents are consistent. Breakdown voltage, field gain coefficient, current and current density, and emitter region (in case of breakdown) are considered in the simulation. Comparison between simulation and experimental results shows that the microstructure has field emitter properties and can be used as a new field emitter.

Keywords: Field emission; fowler-nordheim relation; laser; microstructure; porous silicon.

1. Introduction

The special importance of semiconductors in science and engineering is obvious. There are many scientific reports on this subject by Yang *et al.,* (2010) and Kadim *et al.,* (2022) .Today, silicon and silicon-containing materials have found increasing applications in research and technology see Dubey *et al.,* (2022), Dehghanpour *et al*.,(2010) and Takai *et al.,* (1995*a*). Electron microscopy, X-ray tube and cathode ray tube are examples of field diffusion applications that have been repeatedly investigated in various ways. In addition, the applications of field diffusion matrices for flat plates, electron multipliers and microelectronics were extensively studied by Zhirnof *et al.,* (1995) and Hawley & Zaky ,1967. Local increase of the electric field at the cathode surface leads to diffusion in the microprojects of that surface. Under critical voltage for a group of cathodes, the pre-failure currents depend on the electric field as long as the electric field remains constant. At critical voltage (breakdown voltage), a constant current is converted into a spark. Then, the impedance of the circuit, see Dubey *et al.,* (2022), limits the spark current. An encouraging form of electron source is the cathode field-emitting array (FEA) due to its unique working mechanism and the properties of its cathodic materials. However, there are some significant limitations of small manufacturing FEAs in their performance and accuracy, according Busta *et al.,* (1994). The mentioned disability can be solved in two next ways: development of production techniques and selection of other suitable diffuser materials. Researchers have proposed various types of materials such as carbon nanotubes, Gohier *et al.,* (2007), Rakhi *et al.,*(2008)and Liao *et al.,* (2007), diamond films Lu *et al.,* (2007), Joseph *et al.,* (2008)and Orlanducci *et al.,* (2008), zinc oxide nanowires Yeong & Thong, 2008, Xiao *et al.,* (2008) and Zhang *et al.,* (2006). For the above applications, the optimal conditions are high current density at low extraction voltage and stable performance for cathodes. Due to economic considerations, the use of silicon structures as emitters is particularly attractive. After irradiating hundreds of laser pulses on the silicon surface with

halogen-containing ambient gases, the fabrication of regular self-organizing microstructures (conical microstructures) was reported by Her *et al.,* (1998) and Her *et al.,* (2000). Without any processing operations, the regular conical microstructure showed high and stable field diffusion. Light emission from porous silicon has been extensively investigated. However, its electron field propagation has also been studied by Boswell *et al.,* (1995) and Boswell *et al.,* (1996) as well as according Biaggi-Labiosa *et al.,* (2008). In addition, changes in greenhouse gas emissions due to different porous silicon morphologies have been investigated by Wilshaw & Boswell, 1994. The maximum diffusion current and uniformity of diffusion between different cones can be increased by creating a brittle layer on the silicon wafer using a femtosecond laser as a silicon cone emitter, see Carey *et al.,* (2001). This work provides a model for diffusion of conical microstructure on silicon and experimental results reported by Carey *et al.,* (2001) are used to evaluate the results of the developed model.

2. Theory

Metal surfaces emit electrons at high temperatures T_s or strong electric fields E_s. There are generally three regimes for this phenomenon: (1) the emission of a field where the temperature is low and the electric field is strong, (2) the thermion emission which occurs at high temperatures and weak electric fields, and (3) Heat field (TF) emission, which occurs at high temperatures and strong electric fields. Field diffusion from silicon microstructures (just like metals) is explained in terms of the Fowler-Nordheim relationship, according Reich *et al.,* (2009):

$$j = A\frac{1}{\varphi}E^2 \exp(-\frac{B\varphi^{3/2}}{E}) \quad (1)$$

Here, A and B (properties of the cathode material) are constants that are independent of both the external field (E) and the working function φ. The answer to the problem of quantum mechanics for an electron in an electric field at a good potential is the Fowler-Nordheim equation. The exponential coefficient in Equation (1) determines the transparency of the barrier tunnel D (E), so that j ~ D (E). The height of the barrier is defined by the work function φ, that is, the work that must be done to dissipate electrons from the cathode, and the width of the barrier by the strength of the external field. The work function can be obtained from the experimental relation j (E). The performance of any material (e.g. silicon) can be inferred from non-diffusion phenomena, for example, from optical effect measurements by Groning *et al* (1997). In this case, if current I is uniformly propagated in region A, the density of current j is related to the applied electric field E by the expression of Williams & Williams, 1974:

$$j = \frac{1{\cdot}54 \times 10^{-6}\,\beta^2 E^2}{\varphi\, t^2(y)} \exp\left(-\frac{6{\cdot}83\times 10^7\,\varphi^{3/2} v(y)}{\beta E}\right) \quad (2)$$

Where β and φ represent the working function of the cathode material and the field magnification coefficient (for microprojects on the cathode surface), respectively, and v (y) and t (y) are functions of the variable, see Williams & Williams, 1974:

$$y = \frac{3{\cdot}79 \times 10^{-4}(\beta E)^{3/2}}{\varphi} \quad (3)$$

whose values have been tabulated by Good & Muller, 1956. Equation (2) can be rearranged as, see Williams & Williams, 1974:

$$\frac{I}{E^2} = \frac{1{\cdot}54 \times 10^{-6}\,\beta^2 A}{\varphi\, t^2(y)} \exp\left(-\frac{6{\cdot}83\times 10^7\,\varphi^{3/2} v(y)}{\beta E}\right) \quad (4)$$

Thus, a straight line of m gradient is obtained in the semi-logarithmic diagram ln ($1/E^2$) against 1 / E, where , see Williams & Williams, 1974:

$$m = -\frac{6{\cdot}83\times 10^7\,\varphi^{3/2} s(y)}{\beta} \quad (5)$$

s (y) is another function of the variable y.
Assuming that the work function remains constant, see Williams & Williams, 1974, β is determined from the gradient, and hence the magnitude of the increased breakdown field in the breakdown, Fs (= β Es), may be calculated. Since I_s, the current at which breakdownn begins, is determined from measurements, then from Equations (2) and (3), j_s and A_s, the current density and radiative region at failure are calculated, respectively. Thus, the fracture parameters β, F_s, I_s, j_s and A_s are calculated for each E-I characteristic, and therefore their change is determined by the number of breakdowns for a given set of electrodes.

3. Experiments

On a 3 × 3 mm^2 area on an n-type silicon wafer (800-1200 Ω.cm), a regular self-organizing conical microstructure using 100 femtosecond laser pulses and a raster scan with a flux of 10.9 kJ / m^2 at 100 mm/s was formed. The height of the tiny cones is 10 to 14 mm and they are separated from the tip to the tip of 6 to 10 mm. The voltage applied between the cathode to the anode was in the range of 300 to 1150 volts and measurements were made for the gaps separating the anode from the cathode 20 mm, 40 mm and 60 mm. V-I characteristics were obtained for each separation gap.

4. Simulation

The main purpose of the simulation is to investigate the correlation between the experimental results and the classical field diffusion formula for conical silicon microstructure. An n-type silicon with a 3 × 3 mm^2 microstructure with regular periodic cone arrays (height of cones ~ 10-14 μm, spacing of cones ~ 6-10 μm, tip curvature radius ~ 0.25 μm, tip angles less than 20 °) Intended for simulation. The cathode-anode separation gap was considered to be 20, 40 and 60 μm separately. The applied voltage across the cathode anode is in the range of 300-1100 volts. When using a conical cathode, the equation of the known electric field $E = V / d$ must be modified as, see Gomer (1961):

$$E = \beta V \quad (6)$$

where β is the field magnification factor and is obtained by Gomer (1961):

$$\beta = \frac{1}{kr} \tag{7}$$

where r is radius of the tip curvature and k is given by Gomer (1961):

$$k = 0 \cdot 59 \ \epsilon^{\frac{1}{3}} \left(\frac{x}{r}\right)^{0 \cdot 13} \tag{8}$$

where ϵ is cone's tip angle and x is the cathode-anode separation gap.
An approximation of $v(y)$ in Eq.2 is given as below:

$$v(y) = 1 - n + \frac{1}{6} n ln(n) \tag{9}$$

Where n is obtained by:

$$n = 1 \cdot 43556 \left(\frac{E}{\varphi^2}\right) \tag{10}$$

Where E is the electric field and φ is the work function (for silicon ~ 4.5 eV).

The approximate form of $t(y)$ is as below:

$$t(y) = v(y) - \left(\frac{2y}{3}\right)\left(\frac{d\, v(y)}{dy}\right) \tag{11}$$

After some algebra operations:

$$t(y) = v(y) - \left(\frac{2n}{18}\right)(\ln(n) - 5) \tag{12}$$

5.Results and discussion

Figure 1 shows the voltage-current diagrams for the experimental and simulation results related to the 20 μm cathode-anode separation gap. As we can see, there is a good agreement between the experimental and simulation results at voltages below 1000 volts. Over 1000 V there is a maximum error of ~ 0.5% between the simulation and the experimental results. The threshold voltage for both simulation and experimental results is ~ 600 volts.
The voltage-current diagrams for the simulation and experiments for the 40 μm gap are shown in Figure 2. Again, the experimental results confirm the simulation results with satisfactory accuracy. The maximum error is close to 5%. The field propagation starts with an applied voltage of about 700 volts, which is a logical result due to the expansion of the separation gap. In both figures, there is a nonlinear increase in current against voltage rise, which is consistent with the classical theory of field emitters. This indicates that microstructured silicon behaves like conventional field emitters. This feature and characteristics of silicon semiconductors introduce microstructured silicon as an interesting field emitter.

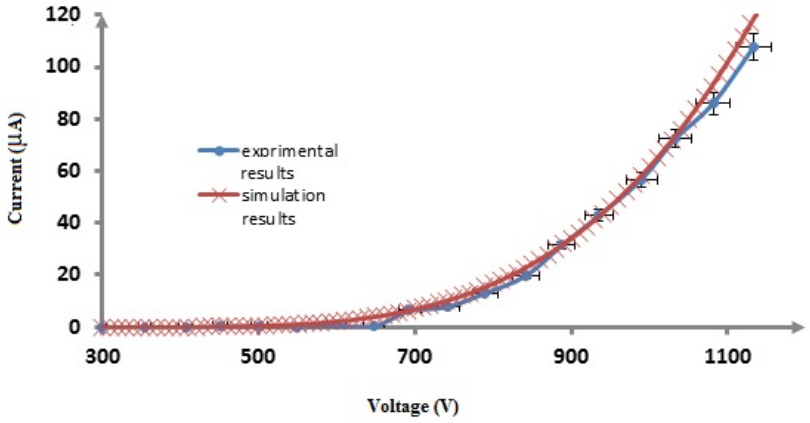

Fig. 1. Voltage-Current diagram with 20 μm cathode-anode separation gap

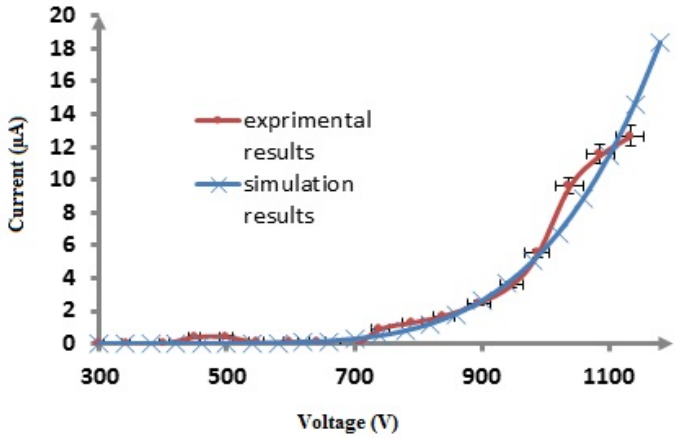

Fig. 2. Voltage-Current diagram with 40 μm cathode-anode separation gap

Figure 3 shows the V-I curves for experimental and simulation results for a 60 μm separation gap between the cathode and anode. The deviation of the experimental results according to the simulation results is greater than this deviation for Figures 1 and 2. The maximum error in the figure 3 is ~ 8%. The threshold voltage is about 800 V. The main reason for this deviation is the significant separation gap for experiment.

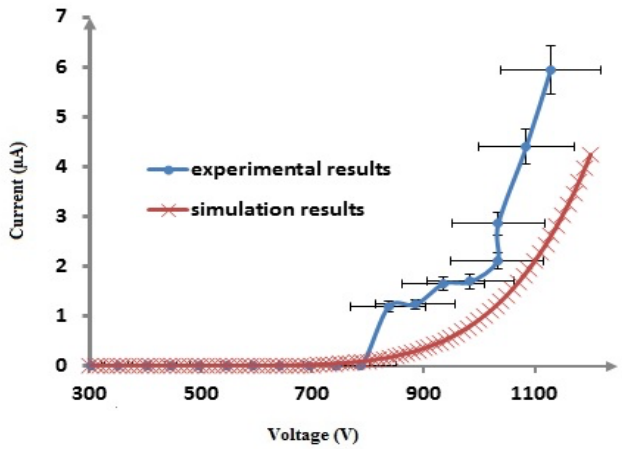

Fig. 3. Voltage-Current diagram with 60 μm cathode-anode separation

The logarithmic form of Equation 4 shows that $ln\ (I/v^2)$ versus v^{-1} is theoretically linear. Then, reviewing the experimental results and simulation with linear forms is an essential task to show the field emitting competence. For this reason, the $ln\ (I/v^2)$ versus v^{-1} diagrams for the 20, 40, and 60 μm separation gaps are summarized in Figures 4-6, respectively. Figure 4 shows the logarithmic form of Equation 4 (Fowler-Nordheim equation) for a gap of 20 μm. Obviously, the experimental results are in good agreement with the linear simulation results in the voltage range of 700 to 1250 volts, but there are significant deviations at voltages below 700 volts. According to Figure 1, the voltage is close to the field emitter threshold voltage and is a logical deviation.

Figure 5 shows the F-N logarithmic equation for the cathode-anode separation gap of 40 μm. The applied voltage range is 600 to 1100 volts. There is a good correlation between the simulation and experimental results, and both results are correlated on a straight line (as predicted by the logarithmic equation F-N). The F-N equation is logarithmically shown in Figure 6 for the 60 μm separation gap. Simulation curves and experimental results have significant deviations. In addition, experimental curves in the form is significantly nonlinear. As before, it is due to the large separation gap (reduction of the electric field strength between the cathode and the anode). There is a maximum deviation of ~ 7 ٪ for the experimental results with respect to the simulation curves.

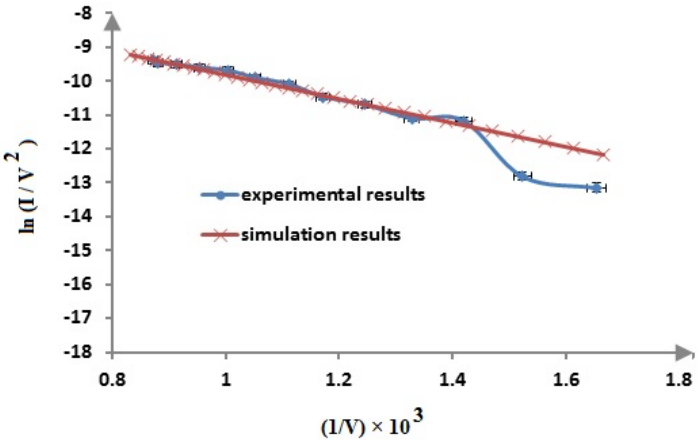

Fig. 4. The logarithmic F-N equation for the cathode- anode separation gap equal to 20 μm

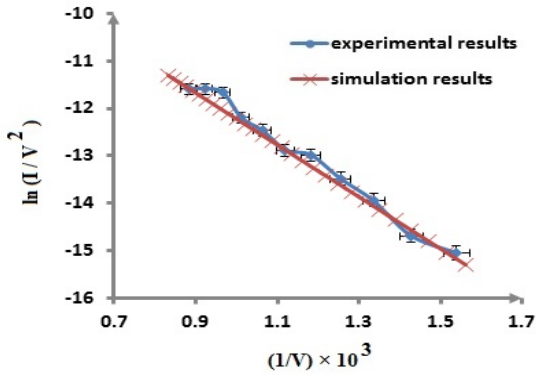

Fig. 5. The logarithmic F-N equation for the cathode- anode separation gap equal to 40 μm

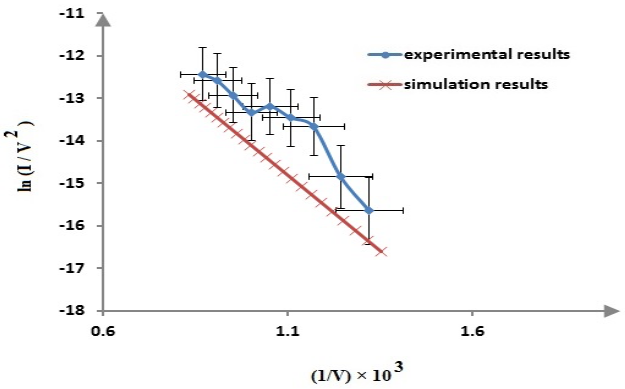

Fig. 6. The logarithmic F-N equation for the cathode- anode separation gap equal to 60 µm

Finally, in order to be more confident in the simulation results, a qualitative comparison with the experimental results of field emission with silicon micro-cones in the last three decades by Evsikov *et al.,* (2012), Prommesberger *et al.,* (2017), Serbun *et al.,* (2013), Ding *et al.,* (2002), Shang *et al.,* (2002), Rangelowa *et al.,*(2001), Colgan & Brett, 2001, Jessing *et al.,*(1998), Rakhshandehroo *et al.,* (1997), Mehr *et al.,* (1996) and Takai *et al.,* (1995 *b*) is collected in Table 1. Because none of the micro-cones tested in these reports were based on the interaction of the laser with the silicon surface and in sulfur hexafluoride atmosphere, a direct comparison with the simulation results was not possible. Therefore, only a qualitative comparison with the trend of the output curves of these works has been considered. However, there is a very good qualitative agreement between the results of the existing experimental work and the simulation results in this work. This shows that the simulation is very reliable.

Table 1. Qualitative comparison of experimental results with emitters including silicon tips with simulation results of the present work

Authors	Field emitter	V-I results	F-N Results	Agreement with the present work
Ilya D. Evsikov *et al* 2021 [30]	Silicon pyramidal microstructures	Nonlinear	Linear	Good
C. Prommesberger *et al* 2017 [31]	p-type Si tip arrays	Nonlinear	Nonlinear	Fair
P. Serbunet al 2013 [32]	p-type silicon tip arrays	Nonlinear	Nonlinear	Fair
M. Ding *et al* 2002 [33]	Silicon tips	Nonlinear	Linear	Reasonable
N. Shang et al 2002 [34]	High density silicon cone arrays	Nonlinear	Linear	Good
I.W. Rangelow & St. Biehl 2001 [35]	Silicon tips	Nonlinear	Nonlinear	Reasonable
M.J. Colgan & M.J. Brett 2001 [36]	Silicon tips	Nonlinear	--------	Good
J. R. Jessing *et al* 1998 [37]	Porous silicon	Nonlinear	Linear	Good
M. R. Rakhshandehroo & S. W. Pang 1997 [38]	Si emitter tips	Nonlinear	---------	Good
W. Mehr *et al* 1996 [39]	Single crystal silicon field emission tip arrays	Nonlinear	Linear	Good
M. Takai *et al* 1995 *b* [40]	n-type porous Si	Nonlinear	Linear	Good

6.Conclusion

The self-organizing regular microstructure on silicon had previously been proposed as a field emitter. In this paper, with a known formulation for field emission, a model for silicon microstructure is introduced and the simulation results are compared with the experimental results. The agreement between the model and the experiment in the small separation gap (40 and 60 μm) between the cathode and the anode is satisfactory. Increasing the separation gap (60μm) leads to a deviation between the model and the experiment. These results indicate that the microstructure on silicon can be used as a field emitter in the cathode-anode separation gap below 50 μm.

References

Biaggi-Labiosa, A. Solá, F. Resto, O. Fonseca, L. González-Berríos, A. De Jesus, J. Morell, G. (2008). Porous silicon field emitter for display applications. Phys. Status Solidi C **5** (11), 3479

Boswell, E. C. Huang, M. Smith, G. D. W. Wilshaw , P. R. (1996). Characterization of porous silicon field emitter properties. J. Vac. Technol. B **14**, 1895

Boswell, E. Seong, T. Y. Wilshaw, P. R. (1995). Studies of porous silicon field emitters. J.Vac. Technol. B **13**, 437

Busta, H. H. Pogemiller, J. E. Zimmerman, B. J. (1994). Scaling of emission currents and of current fluctuations of gated silicon emitter ensembles. J. Vac. Sci. Technol. B **12**, 689

Carey, J. E. Zhao, L. Crouch, C. Wu, C. Mazur, E. (2001). Field Emission from Silicon Microstructures Formed by Femtosecond Laser Assisted Etching. Proc. CLEO Baltimore, MD, 555-557

Colgan, M.J. Brett, M.J. (2001). Field emission from carbon and silicon films with pillar microstructure. Thin Solid Films **389**, 1

Dehghanpour H. R. Parvin, P. (2010). Fluorine penetration into amorphous SiO2 glass at SF6 atmosphere using Q-switched Nd: YAG and excimer laser irradiations, Jpn. J. Appl. Phys. **49** (7R): 07580.

Ding, M. Sha,G. Akinwande, A. I. (2002). Silicon Field Emission Arrays With Atomically Sharp Tips: Turn-On Voltage and the Effect of Tip Radius Distribution. IEEE Trans. Elec. Devices **49**(12), 2333

Dubey, R.S., Venkatesh, Y. (2022). Engineering of Ultra-Violet Reflectors byvarying Alternate Layers of Titania/Silica for Harmful UV-Protection, Kuwait J. Sci. KJS - Online-First Articles, DOI: 10.48129/kjs.16633

Evsikov, I. D. , Demin,.G. D. Gryazneva, T. A. Makhiboroda, M. A. Djuzhev N. A. Pankratov, O. V. Popov E.O. Filippov, S.V. . Kolosko A. G. Chumak, M. A. (2021). Experimental study of the multi-tip field emitter based on the array of silicon pyramidal microstructures. 34th International Vacuum Nanoelectronics Conference (IVNC).

Gohier A, Djouadi M A, Dubosc M, Granier A, Minea T M, Sirghi L, Rossi F, Paredez P and Alvarez F. (2007). Single- and Few-Walled Carbon Nanotubes Grown at Temperatures as Low as 450 °C: Electrical and Field Emission Characterization. *J.* Nanosci. Nanotechnol. **7**(9), 3350

Gomer, R. (1961) Field emission and field ionization. Harvard Monographs In Applied Science No 9. **Cambridge**, Massachusetts.

Good, R.H., Muller, E.W. (1956). Handbook of Physics. Springer-Verlag, **Berlin**
Groning, O. Kuttel, O. Groning, M. Groning, P. Schlapbach, L. (1997). Field emitted electron energy distribution from nitrogen-containing diamondlike carbon. Appl. Phys. Lett. **71**, 2253

Hawley, R. Zaky, A. A. (1967). Progress in Dielectrics. Vol. **7**. pp. 115-215. Heywood, London

Her, T. H. Finlay, R.J. Wu, C. Mazur, E. (2000). Femtosecond laser-induced formation of spikes on silicon. Appl. Phys. A **70**, 383

Her, T.H. Finlay, R.J. Wu, C. Deliwala, S. Mazur, E. (1998). Microstructuring of silicon with femtosecond laser pulses. Appl. Phys. Lett. **73**, 1673

Jessing, J. R. Kim, H. R. Parker, D. L. Weichold M. H. (1998). Fabrication and characterization of gated porous silicon cathode field emission arrays. J. Vac. Sci. Technol. B **16** (2), 777

Joseph, P. T. Tai, N. H. Lee, C. Y. Niu, H. Pong, W. F. Lin, I. N. (2008). Field emission enhancement in nitrogen-ion-implanted ultrananocrystalline diamond films. J. Appl. Phys. **103**, 043720

Kadim A. (2022). Fabrication of Nano Battery from CdS Quantum Dots and Organic Polymer, Kuwait J. Sci. **49** (1): 1-9.

Liao, L. Lie, J. C. Liu, C. Xu, Z. Wang, W. L. Liu, S. Bai, X. D. Wang, E. G. (2007). Field Emission of GaN-Filled Carbon Nanotubes: High and Stable Emission Current. J. Nanosci. Nanotechnol. **2** (11), 2875

Lu, X. Yang, Q. Xiao, C. Hirose, A. (2007). Effects of hydrogen flow rate on the growth and field electron emission characteristics of diamond thin films synthesized through graphite etching. Diam. Relat. Mater. **16** (8), 1623

Mehr, W. Wolff, A. Frankenfeld, H. Skaloud, T. Hoppner, W. Bugiel, E. Lgrz, J. Hunger, B. (1996). Ultra sharp crystalline silicon array used as field emitter. Microelec. Engin. **30**, 395

Orlanducci, S. Fiori, A. Sessa, V. Tamburri, E. Toschi, F . Terranova, M. L. (2008). Nanocrystalline Diamond Films Grown in Nitrogen Rich Atmosphere: Structural and Field Emission Properties. J. Nanosci. Nanotechnol. **8**(6), 3228

Prommesberger, C. Langer, C. Lawrowski, R. Schreiner, R. (2017). Investigations on the long-term performance of gated p-type silicon tip arrays with reproducible and stable field emission behavior. J. Vac. Sci. Technol. B **35**(1), 012201-1

Rakhi, R. B. Sethupathi, K. Ramaprabhu, S. (2008). Field emission from carbon nanotubes on a graphitized carbon fabric. Carbon. https://doi.org/10.1016/j.carbon.2008.07.024.

Rakhshandehroo, M. R. Pang, S. W. (1997). Field emission from gated Si emitter tips with precise gate–tip spacing, gate diameter, tip sharpness, and tip protrusion. J. Vac. Sci. Technol. B **15**(6), 2777

Rangelowa, I.W. Biehlb, St. (2001). High aspect ratio silicon tips field emitter array. Microelec. Engin.**57–58**, 613

Reich, K. V. Eidelman, E. D. (2009). Effect of electron-phonon interaction on field emission from carbon nanostructures. Euro. Phys. Lett. **85**(4), 47007

Serbun, P. Bornmann, B. Navitski, A. Muller G. (2013). Stable field emission of single B-doped Si tips and linear current scaling of uniform tip arrays for integrated vacuum microelectronic devices. J. Vac. Sci. Technol. B **31**(2), 02B101-1

Shang, N. G. Meng, F. Y. Au, F. C. K. Li, Q. Lee, C. S. Bello, I. Lee, S. T. (2002). Fabrication and field emission of high density silicon cone arrays. Adv. Mater. **14**(18), 1308

Takai, M. Yamashita, M. Wille, H. (1995*a*). Enhancement in emission current from dry-processed n-type Si field emitter arrays after tip anodization. J. Vac. Sci. Technol. B **13** (2), 441

Takai, M. Yamashita, M. Wille, H. Yura, S. Horibata,S. Ototake, M., (1995*b*). Enhanced electron emission from n-type porous Si field emitter arrays Appl. Phys. Lett.. **66**, 422

Williams, D. W. Williams, W. T.(1974). Pre-breakdown and breakdown characteristics of stainless steel electrodes in vacuum. J. Phys. D: Appl. Phys. **7**(8), 1173

Wilshaw, P. R. Boswell, E. (1994). Field emission from pyramidal cathodes covered in porous silicon. J. Vac. Sci. Technol. B **12**, 662

Xiao, J. Zhang, G. M. Bai, X. Yu, L. G. Zhao, X. Y. Guo, D. Z. (2008). Field emission from zinc oxide nanostructures and its degradation. Vacuum. **83**(2), 265

Yang, Y., McDowell, M., Jackson, A., Cha, J., Hong, S., and Cui, Y., (2010). New nanostructured Li2S/silicon rechargeable battery with high specific energy. Nano Lett., **10**: 1486–1491

Yeong, K. S. Thong, J. T. L. (2008). Field emission properties of individual zinc oxide nanowire field emitter. J. Vac. Sci. Technol. B **26**, 983

Zhang, Y. S., Yu, K. Ouyang, S. X. Zhu, Z. Q. (2006). Selective-area growth and field emission properties of Zinc oxide nanowire micropattern arrays. Phys. B **382**(1-2), 76

Zhirnof, V. V. Givargizov, E.I. Plekhanov, P.S. (1995). Field emission from silicon spikes with diamond coatings. J. Vac. Sci. Technol. **13**, 418

Submitted: 06/11/2021
Revised: 15/02/2022
Accepted: 20/02/2022
DOI: 10.48129/kjs.17069